

available at www.sciencedirect.comjournal homepage: www.elsevier.com/locate/carbon

Controllable melting and flow of β -Sn in flexible amorphous carbon nanotubes

Xinyong Tao^a, Lixin Dong^b, Wenkui Zhang^{a,*}, Xiaobin Zhang^{c,*}, Jipeng Cheng^c, Hui Huang^a, Yongping Gan^a

^aCollege of Chemical Engineering and Materials Science, Zhejiang University of Technology, Hangzhou 310014, China

^bDepartment of Electrical and Computer Engineering, Michigan State University, 2120 Engineering Building, East Lansing, MI 48824, USA

^cDepartment of Materials Science, Zhejiang University, Hangzhou 310027, China

ARTICLE INFO

Article history:

Received 7 June 2009

Accepted 9 July 2009

Available online 15 July 2009

ABSTRACT

A high-yield of carbon nanotubes filled with β -Sn nanowires has been produced by the thermal pyrolysis of acetylene over SnO_2 catalysts. Electron beam irradiation (EBI) induced melting and flow of Sn in the nanotubes and this could be controlled by changing the electron beam current density. The mass flow rate of the Sn ranged from 0.9 to 8.2 fg/s. The melting of the nanowires is a result of the temperature rise caused by the EBI. Many factors, including temperature variation, charging, and EBI induced deformation of the carbon shells, contribute to the flow of Sn.

© 2009 Elsevier Ltd. All rights reserved.

1. Introduction

Carbon nanotubes (CNTs) exhibit remarkable structural, mechanical, and electronic properties. Among these characteristics, the hollow cavity allows the encapsulation of a variety of metals which have been predicted and found to lead to novel structures and properties. Therefore, metal-filled CNTs have attracted tremendous attention due to their potential applications in nanoelectronics and nanoelectromechanical systems (NEMs) such as nanoextruders [1], electrical nanocables [2], nanomagnets [2], nanoswitches [3], nanothermometers [4], and nano test tubes [5].

To date, several methods of encapsulating metals within CNTs have been developed including wet chemical methods [6], capillary action [7,8], arc-discharge techniques [9], catalyzed hydrocarbon pyrolysis [2], condensed-phase electrolysis [10–13], and electrocapillary-driven filling [14]. Metals, such as Ti, Cr, Fe, Co, Ni, Cu, Ga, In, Zn, Mo, Pd, Ta, W, Gd, Dy, Yb, Sn, Hg, and Fe–Co [1–16], have been encapsulated into CNTs. Hsu et al. prepared graphite carbon sheathed Sn and Sn–Pb nanowires by an electrolytic technique [10–13]. Li et al. prepared Sn-filled CNTs by thermal evaporation of solid Sn powder

and thermal pyrolysis of ethylene gas (C_2H_2) [17]. However, all these methods suffer from the low filling fraction and the low yield of filled nanotubes. In this work, a new kind of high-yield CNTs filled with β -Sn nanowires (Sn@CNTs) were produced by a chemical vapor deposition (CVD) method. Different from the normal CNTs with concentric graphite shells, these Sn@CNTs have amorphous carbon structures. Moreover, to be best of our knowledge, we observed for the first time an electron beam irradiation (EBI) induced melting and flow behavior. Due to these unique properties, this new kind of Sn@CNTs show fascinating potentials for NEMs including EBI current density sensors, nanoswitches, nanosolders, nanoclampers, nanorelays, and nanomanipulators.

2. Experimental

2.1. Synthesis of Sn@CNTs

Sn@CNTs were synthesized by catalytic deposition of acetylene using SnO_2 as catalyst. A one-step CVD method was adopted for the synthesis of Sn@CNTs, i.e., the catalyst was directly introduced into the hot furnace without a preheating and reduction

* Corresponding authors. Fax: +86 571 88320394.

E-mail addresses: msechem@zjut.edu.cn (W. Zhang), zhangxb@zju.edu.cn (X. Zhang).

0008-6223/\$ - see front matter © 2009 Elsevier Ltd. All rights reserved.

doi:10.1016/j.carbon.2009.07.032

process. A typical synthesis was as follows: a furnace containing a quartz tube, (external diameter: 60 mm; length: 1200 mm) was heated to 610 °C. Then, to expel air, N₂ was sent through the tube at a flow rate of 600 ml/min for 4 min. Next, a quartz boat, 200 mm long and 30 mm wide, in which ca. 2 g catalyst was uniformly distributed, was inserted immediately in the center of the quartz tube. Subsequently, a mixture of C₂H₂:N₂ = 100:200, v/v, at a flow rate of 300 ml/min was introduced into the quartz tube. The reaction was maintained for 5, 10 and 30 min, after which the furnace was allowed to cool to room temperature under N₂ atmosphere. All gases are introduced into the reactor by the mass flow controller.

2.2. Characterization and the EBI

The product was analyzed by field emission scanning electron microscopy (FESEM, FEI Sirion), transmission electron microscopy (TEM, JEM-200CX, JEM-2010, CM20, and JEM-4000EX), high-resolution transmission electron microscopy (HRTEM), energy-dispersive X-ray spectroscopy (EDS), selected area electron diffraction (SAED), and X-ray diffraction (XRD). The EBI was performed under accelerating voltages of 80–400 kV (JEM-200CX, JEM-2010, CM20, and JEM-4000EX). The critical current densities, which are defined as the minimum beam current density needed to keep a nanowire in a molten state, were measured by changing the focus (beam diameter and brightness) of the electron beam and the accelerating voltage.

3. Results and discussion

3.1. Electron microscopy characterization

A representative FESEM image of Sn@CNTs is shown in Fig. 1a. The CNTs have a diameter distribution from 20 to

80 nm. The TEM image (Fig. 1b) reveals uniform core-sheath structures. The EDS spectra of samples only display Sn and carbon. Six months of exposure to air at room temperature results in no oxygen signals in the EDS spectra (inset in Fig. 1b), indicating that CNTs provide an effective barrier against oxidation and consequently ensure long-term stability of the Sn nanowires. A representative HRTEM image (Fig. 1c) shows that the thickness of the carbon layer is ca. 5 nm. The SAED pattern (inset in Fig. 1c) and the locally magnified HRTEM image (Fig. 1d) demonstrate the Sn nanowire is single crystal with a good crystallization. Different from the Sn-filled graphite CNTs synthesized by Hsu et al. [10–13], these CNTs consist of disordered carbon sheets. Small areas of roughly aligned graphite can also be observed (Fig. 1d).

3.2. XRD characterization

In order to understand the growth process of Sn@CNTs, different reaction time using the same catalyst were designed, and the products, specially the evolution of the catalyst during the initial growth stage, were examined by XRD. Fig. 2 is the XRD spectrum of the products synthesized by using different reaction times. It clearly shows phase transformations occur during the reaction process. All the peaks in Fig. 2a can be indexed as SnO₂ (JCPDS 77-0447). After 5 min of reaction, some main peaks of β-Sn (JCPDS 86-2265) appear with very weak intensity (Fig. 2b). TEM results show that some carbon coated β-Sn nanowires can be found in the product synthesized after 5 min of reaction (not shown). It can also be found that the intensity of peaks of β-Sn increase with the reaction time (Fig. 2c). After 30 min, only the peaks of β-Sn can be identified (Fig. 3d), indicating that all the Sn⁴⁺ has been reduced into Sn⁰. Due to the poor crystallization of CNTs, it cannot be identified the (0 0 2) peak in the

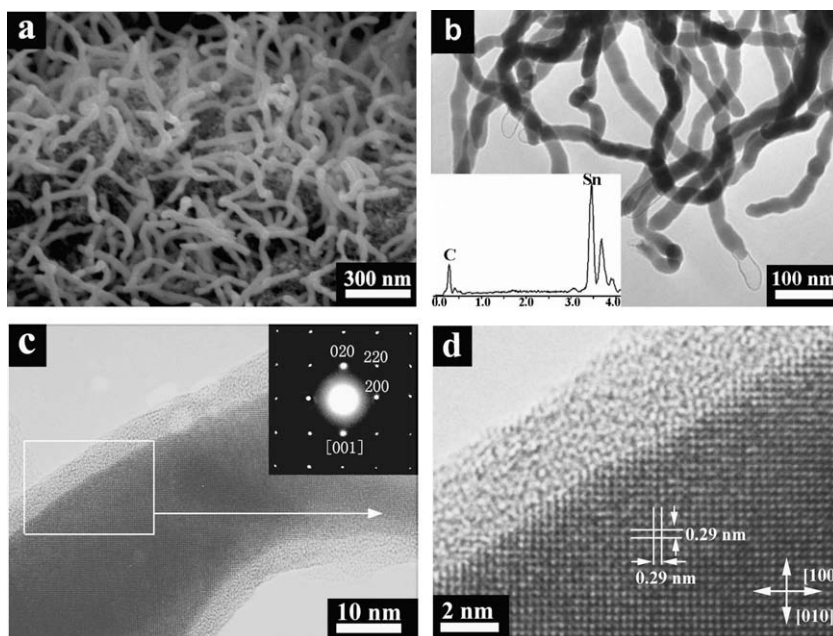


Fig. 1 – (a) FESEM and (b) TEM images of Sn@CNTs synthesized at 610 °C for 30 min, the inset is a representative EDS spectrum; (c) HRTEM image of Sn@CNTs, the inset in the top right corner is the corresponding SAED pattern along the [0 0 1] crystallographic direction of tetragonal β-Sn and (d) the locally magnified HRTEM image.

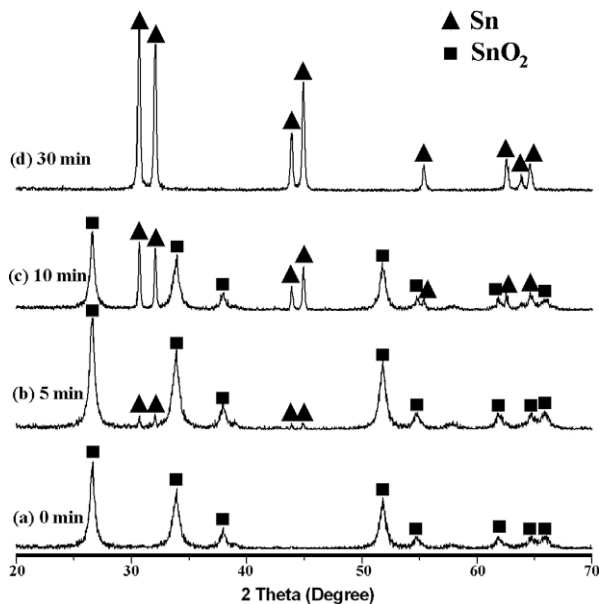


Fig. 2 – XRD spectrums of products synthesized with different reaction time.

XRD spectrum. In the previous reports of metallic In [16] and Ga [4] filled CNTs, a two-step growth mechanism was proposed to explain the formation of carbon sheathed In and Ga nanowires, in which the suboxide Ga_2O and In_2O play key roles in the catalytic decomposition of carbon source. It is worthy noting that not any suboxide SnO was detected in our case, indicating that the catalyst for the growth of the carbon coated β -Sn nanowires was not SnO. In order to understand the growth mechanism further, the β -Sn and SnO nanocrystals were used as catalyst instead of SnO_2 . No CNTs filled with β -Sn nanowires can be obtained using both β -Sn and SnO as catalyst. Based on our experimental results, it can be concluded that the formation of the carbon coated β -Sn nanowires is a one-step process, i.e., the formation of the carbon coated β -Sn nanowires is simultaneous with the reduction of SnO_2 .

3.3. EBI induced melting and flow

A striking phenomenon was the observation of thermometer-like melting and flow of Sn within CNTs when the

Sn@CNTs were supported on an insulated substrate and irradiated under different EBI energy (80, 100, 120, 160, 200 and 400 kV) within transmission electron microscopes. Fig. 3 shows the TEM image sequence of a Sn nanowire under EBI with different current density. TEM analyses show that the Sn nanowire has no any morphological change when the current density is lower than 0.3 A/cm^2 (see Fig. 3a). But the nanowire melts entirely in a high speed and starts moving along the wire axis when the current density reaches 0.4 A/cm^2 (Fig. 3b). More interesting, an expansion and contraction behavior accompanied with the increasing and decreasing current density can be found (see Fig. 3b–i). A large number of TEM analyses proved that this kind of expansion and contraction process was reversible and simultaneous with the change of EBI current density.

Many studies have been conducted on various phase transformation in metal and alloy by TEM, including the melting and solidification behavior [1,4,16,18–21]. Melting occurs when the amplitude of the thermal vibrations of atoms in a material reaches a certain fraction of the lattice constant and the distance between the atoms exceeds a critical length [21]. Therefore, melting under electron irradiation is expected to result from inelastically scattering induced temperature rise and/or the displacement of atoms caused by the incident electrons [19,21]. These effects are discussed in the following.

The displacement energy E_d is the kinetic energy required to displace an atom from its original lattice position to an unstable one. The displacement cross section σ_d , which represents the probability that an electron with energy E_p can displace an atom as the area of a target, is given by [21,22]

$$\sigma_d = z^2 4\pi a_0^2 U_R^2 \left(\frac{1 - \beta^2}{m^2 c^4 \beta^4} \right) \left[\frac{E_{\max}}{E_d} + 2\pi\alpha\beta \sqrt{\frac{E_{\max}}{E_d}} - (\beta^2 + \pi\alpha\beta) \right] \times \ln \left(\frac{E_{\max}}{E_d} \right) - (1 + 2\pi\alpha\beta) \quad (1)$$

where $E_{\max} = 2E_p(E_p + 2mc^2)/Mc^2$, M is the mass of the nucleus, a_0 is the Bohr radius ($5.29 \times 10^{-11} \text{ m}$), U_R is the Rydberg energy (13.6 eV), Z is the atomic number of the nucleus, and $\alpha = Z/137$. The incident electron energy E_p is determined from the equation $E_p = mc^2 [(1 - \beta^2)^{1/2} - 1]$, where m is the rest mass of the electron, c is the speed of light, v is the velocity of the electron, and $\beta = v/c$. Fig. 4 is the calculated displacement cross section of Sn as a function of the incident electron energy. The E_d of Sn is 22 eV [23], the σ_d decreases as the incident

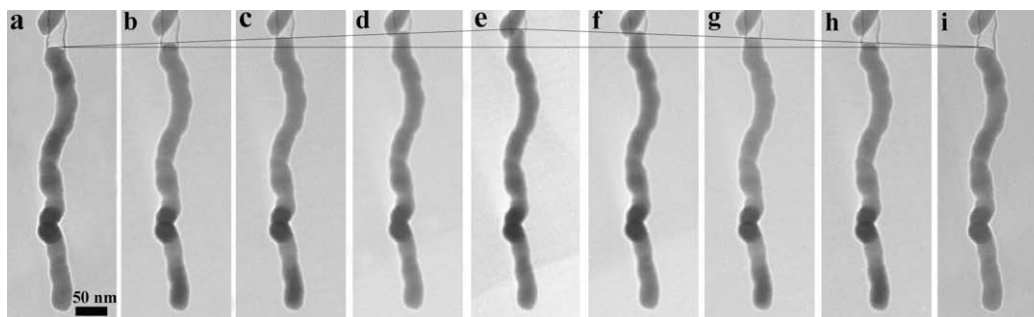


Fig. 3 – The TEM image sequence of the Sn@CNT irradiated with increasing EBI current density: (a) 0.1 A cm^{-2} , (b) 0.4 A cm^{-2} , (c) 1.5 A cm^{-2} , (d) 2.4 A cm^{-2} , (e) 3.5 A cm^{-2} ; and decreasing EBI current density: (f) 2.4 A cm^{-2} , (g) 1.5 A cm^{-2} , (h) 0.4 A cm^{-2} , and (i) 0.1 A cm^{-2} .

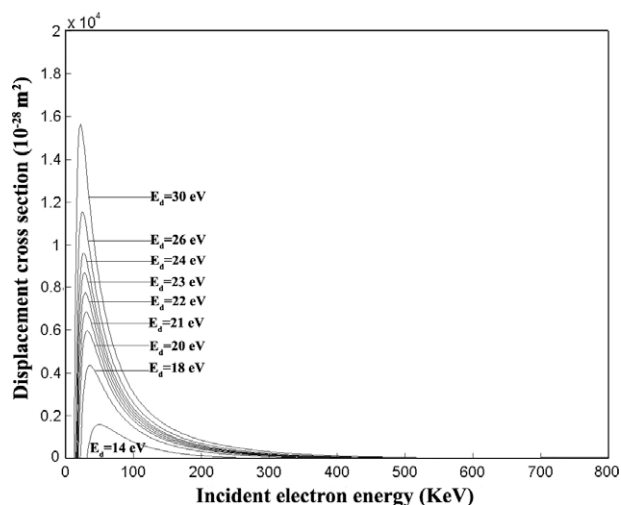


Fig. 4 – Variation of the displacement cross section with incident electron energy for a series of displacement energies around that of Sn.

electron energy increases from 50 to 400 keV and it decreases very rapidly at low incident electron energy (Fig. 4). If atomic displacements are dominating the melting of Sn nanowires, the occurrence probability of the melting will decrease with the increase of the accelerating voltage in the range from 80 to 400 kV (see Fig. 4). In our experiments, it was found that the Sn nanowires can be melted under the irradiation of electron beam with different energy including 80, 100, 120, 160, 200, and 400 keV. The EBI experiments proved that the melting occurred with equal probability under different accelerating voltages. It means that atomic displacements are not causing the nanowire to melt, although they do occur in the nanowire. It is concluded that the temperature rise caused by the EBI results in the melting of the nanowires. TEM experiments also proved that the melting of the nanowires deposited on SiO_x TEM grids was preferential compared with the nanowires on carbon TEM grids, which resulted from the poor thermal conductivity of the SiO_x substrate.

A possible question arises: Is it a kind of heat expansion and cold contraction behavior in Fig. 3? The coefficient of

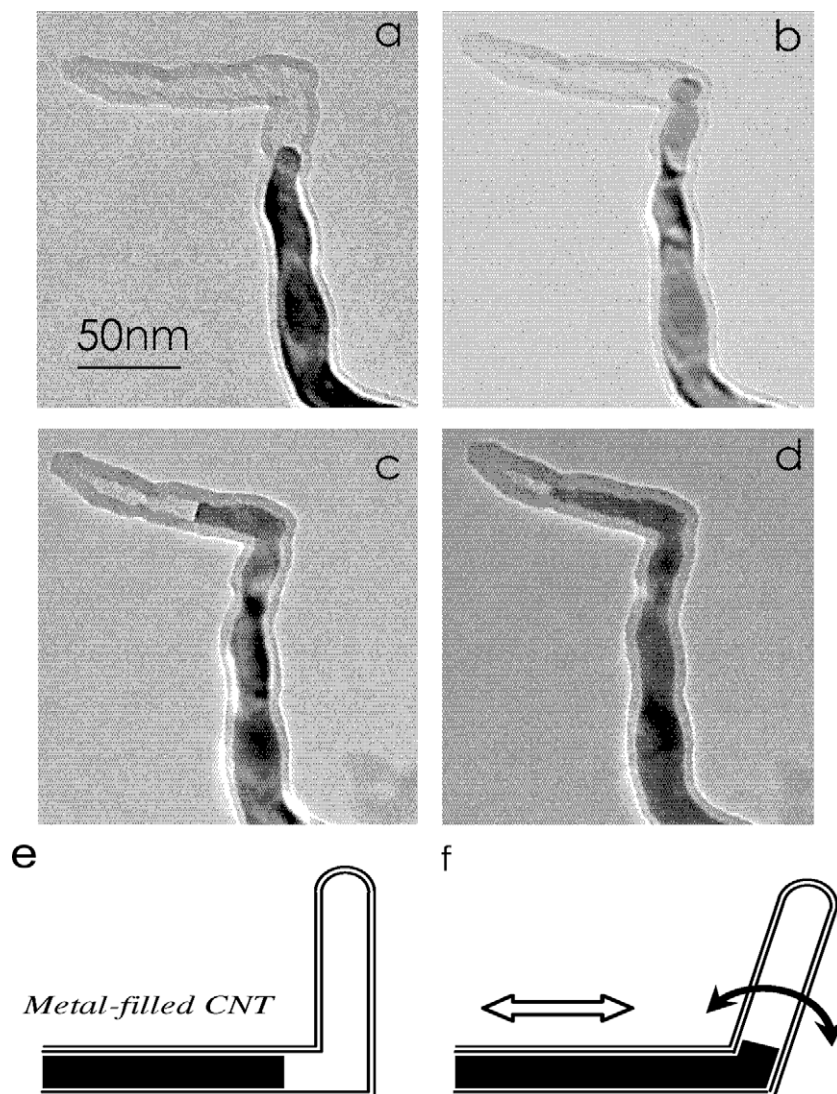


Fig. 5 – (a–d) Electron beam induced flow straightens a kinked Sn@CNT. (e and f) This kind of flow induced deformation can find potential applications as nanogrippers, nanoswitches, or nanomanipulators.

volume expansion of Sn is $106 \times 10^{-6} \text{ }^\circ\text{C}^{-1}$ [24]. TEM results showed that there was no obvious shrinkage in the carbon shell. Suppose the volume change of the carbon shell is 0, the maximum volume increase in Fig. 3 will be 7.4%. If the flow behavior belongs to heat expansion and cold contraction, the corresponding temperature increase will be about 698 °C. Many reports have proved that the temperature rise induced by the EBI is about 50–100 °C [25,26], which is far lower than 698 °C. It is believed that, besides the heat effect resulting from the EBI, many other factors do contribute to the flow. One is the charging of the specimen system. If a metal sample is sitting on the substrate such as SiO_x TEM grids, which is not good conductor of electricity, the sample will be charged positively because the emission of secondary electrons by EBI [26]. This charging will impose Coulomb repulsive forces on the samples or local areas of the substrate [26]. Iijima and Ichihashi proved that this kind of EBI induced charging resulted in structural instability of metal nanoparticles [26]. Golberg et al. revealed that the EBI induced charging caused the melting, expansion and/or sudden shrinkage of the liquid indium inside silica nanotubes [18]. The other possible factor is the EBI induced deformation of carbon shell [1]. Carbon onions and CNTs have been shown to act as a self-contracting high-pressure cell under EBI [1]. Controlled EBI of multi-walled CNTs can cause large pressure buildup within the nanotube cores that can deform and extrude the metals inside the CNTs [1]. The appearance of the meniscus (Fig. 3b–h) indicates that the flow of liquid Sn is not related to the wetting effect. TEM results proved that the mass flow rate of the Sn ranged from 0.9 to 8.2 fg/s, which can be controlled by changing the switch rate of the current density. Based on this unique melting and flow phenomena, this kind of Sn@CNTs can be used as the EBI current density sensor in TEM, nanosolders, etc.

3.4. Flow induced deformation of CNTs

When a kinked Sn@CNT was exposed to the e-beam of TEM, an interesting flow induced deformation of carbon shell like what happens in a soft water pipe was observed (Fig. 5). In the whole process, a 12° deflection of the junction is observed, which induced a ca. 35 nm displacement at the free-standing tip of the nanotube (the arm length of the horizontal tube is ca. 110 nm). This flow induced deformation indicates that these amorphous carbon shells are flexible, which is different from the normal graphite CNTs. With its ultra-compact sizes, such nanotube-based fluidic junctions can be potentially used as actuators for creating nanorelays, nanogrippers, nanoswitches, or nanomanipulators (Fig. 5e and f). Further investigations are undergoing for improving the controllability using EBI-driven mechanism.

4. Conclusions

High-yield amorphous flexible CNTs filled with β-Sn nanowires were synthesized by a one-step CVD method. The Sn nanowires can be melted under the irradiation of electron beam in TEM. A unique thermometer-like flow behavior accompanied with the change of current density was found.

The temperature rise caused by the EBI results in the melting of the nanowires. Besides the heat effect resulting from the EBI, many other factors including charging and EBI induced deformation of carbon shells do contribute to the flow of Sn. Based on this new phenomena, this kind of Sn@CNTs is expected to find applications in EBI current density sensors, nanoswitches, nanosolders, nanoclampers, nanorelays, and nanomanipulators, etc.

Acknowledgements

Financial support for this study was provided by the national natural science foundation of China (No. 50571087). The authors thank Dr. Yu Li for TEM technical support.

REFERENCES

- [1] Sun L, Banhart F, Krashennnikov AV, Rodriguez-Manzo JA, Terrones M, Ajayan PM. Carbon nanotubes as high-pressure cylinders and nanoextruders. *Science* 2006;312:1199–202.
- [2] Elias AL, Rodriguez-Manzo JA, McCartney MR, Golberg D, Zamudio A, Baltazar SE, et al. Production and characterization of single-crystal FeCo nanowires inside carbon nanotubes. *Nano Lett* 2005;5:467–72.
- [3] Dorozhkin PS, Tovstonog SV, Golberg D, Zhan JH, Ishikawa Y, Shiozawa M, et al. A liquid-Ga-fitted carbon nanotube: a miniaturized temperature sensor and electrical switch. *Small* 2005;1:1088–93.
- [4] Gao YH, Bando Y. Carbon nanothermometer containing gallium – gallium's macroscopic properties are retained on a miniature scale in this nanodevice. *Nature* 2002;415:599.
- [5] Ugarte D, Chatelain A, deHeer WA. Nanocapillarity and chemistry in carbon nanotubes. *Science* 1996;274:1897–9.
- [6] Tsang SC, Chen YK, Harris PJF, Green MLH. A simple chemical method of opening and filling carbon nanotubes. *Nature* 1994;372:159–62.
- [7] Ajayan PM, Ebbesen TW, Ichihashi T, Iijima S, Tanigaki K, Hiura H. Opening carbon nanotubes with oxygen and implications for filling. *Nature* 1993;362:522–5.
- [8] Ajayan PM, Iijima S. Capillarity-induced filling of carbon nanotubes. *Nature* 1993;361(6410):333–4.
- [9] Subramoney S. Novel nanocarbons – Structure, properties, and potential applications. *Adv Mater* 1998;10:1157–71.
- [10] Hsu WK, Hare JP, Terrones M, Kroto HW, Walton DRM, Harris PJF. Condensed-phase nanotubes. *Nature* 1995;377:687.
- [11] Hsu WK, Li J, Terrones H, Terrones M, Grobert N, Zhu YQ, et al. Electrochemical production of low-melting metal nanowires. *Chem Phys Lett* 1999;301:159–66.
- [12] Hsu WK, Terrones M, Terrones H, Grobert N, Kirkland AI, Hare JP, et al. Electrochemical formation of novel nanowires and their dynamic effects. *Chem Phys Lett* 1998;284:177–83.
- [13] Hsu WK, Trasobares S, Terrones H, Terrones M, Grobert N, Zhu YQ, et al. Electrolytic formation of carbon-sheathed mixed Sn–Pb nanowires. *Chem Mater* 1999;11:1747–51.
- [14] Chen JY, Kutana A, Collier CP, Giapis KP. Electrowetting in carbon nanotubes. *Science* 2005;310:1480–3.
- [15] Cheng HM. Structure and application of carbon nanotube. Beijing: Chemical Industry Press; 2002.
- [16] Gao YH, Bando Y, Golberg D. Melting and expansion behavior of indium in carbon nanotubes. *Appl Phys Lett* 2002;81:4133–5.

- [17] Li RY, Sun XC, Zhou XR, Cai M, Sun XL. Aligned heterostructures of single-crystalline tin nanowires encapsulated in amorphous carbon nanotubes. *J Phys Chem C*. 2007;111:9130–5.
- [18] Golberg D, Li YB, Mitome M, Bando Y. Real-time observation of liquid Indium unusual behavior inside silica nanotubes. *Chem Phys Lett* 2005;409:75–80.
- [19] Lereah Y, Kofman R, Penisson JM, Deutscher G, Cheyssac P, Ben-David T, et al. Time-resolved electron microscopy studies of the structure of nanoparticles and their melting. *Philos Mag B* 2001;81:1801–19.
- [20] Liu J, Barbero CJ, Corbett JW, Rajan K, Leary H. An in situ transmission electron-microscopy study of electron-beam-induced amorphous-to-crystalline transformation of Al_2O_3 films on silicon. *J Appl Phys* 1993;73:5272–3.
- [21] Yokota T, Murayama M, Howe JM. In situ transmission-electron-microscopy investigation of melting in submicron Al–Si alloy particles under electron-beam irradiation. *Phys Rev Lett* 2003;91:265504.
- [22] Banhart F. Irradiation effects in carbon nanostructures. *Rep Prog Phys* 1999;62:1181–221.
- [23] Nastasi M, Mayer JW, Hirvonen JK. Ion-solid interactions fundamentals and applications. New York: Cambridge University Press; 2004.
- [24] Metallurgy and metallic materials. Beijing: Chemical Engineering Press; 2001.
- [25] Du XW, Wang B, Zhao NQ, Furuya K. Structure evolution of silicon nanocrystals under electron irradiation. *Scr Mater* 2005;53:899–903.
- [26] Iijima S, Ichihashi T. Structural instability of ultrafine particles of metals. *Phys Rev Lett* 1986;56:616–9.